Electronic Supplementary Material (ESI) for RSC Advances.

Supporting Information

Structure-Property Relationship of Two Structural Isomers of Thiophene-Flanked Diazaisoindigo on Carrier Transport Properties.

Minoru Ashizawa,[a,*] Tsukasa Hasegawa,[a] Susumu Kawauchi,[a] Hiroyasu Masunaga,[b] Takaaki Hikima,[c] Hiroyasu Sato,[d] and Hidetoshi Matsumoto[a,*]

[a]*Department of Materials Science and Engineering, Tokyo Institute of Technology, O-okayama 2-12-1, Meguro-ku, Tokyo 152-8552, Japan.*

[b]*Japan Synchrotron Radiation Research Institute (JASRI)/SPring-8, 1-1-1 Kouto, Sayo, Sayo 679-5198, Japan*

[c]*RIKEN SPring-8 Center, 1-1-1 Kouto, Sayo, Sayo 679-5148, Japan*

Corresponding Authors

ashizawa.m.aa@m.titech.ac.jp

I. General

All the chemicals and solvents were of reagent grade purchased from Tokyo Kasei Chemical Industries, Wako Pure Chemical Industries, and Aldrich and used without further purification. All reactions were carried out under an argon atmosphere. The ^{1}H and ^{13}C NMR spectra were recorded using a JEOL JNM-AL300 spectrometer (300 MHz) in deuterated chloroform at 298 K and tetramethylsilane was used as the internal standard. Mass spectrograms were recorded by a Shimadzu QP-5000 (EI-MS) or Shimadzu MALDI-AXIMA time of flight mass spectrometer (MALDI-TOF) operated in the linear mode. The UV-Vis-NIR absorption spectra of the dilute solution and spin-coated thin film of the present compounds were collected using a Jasco Corporation V-630 UV-VIS-NIR spectrophotometer. The optical energy gaps E_g^{opt} were estimated from the low-energy band edge of the absorption spectra of the thin films. Elemental analyses were performed at the Center for Advanced Materials Analysis, Tokyo Institute of Technology.

II DFT calculations

Density Functional Theory (DFT) calculations were performed using the Gaussian 09 program[1] based on the ωB97X-D/6-31G(d,p) for calculation of the optimized molecular geometry and ground-state electronic structures and ωB97X-D/6-311++G(d,p) for TD-DFT calculation.

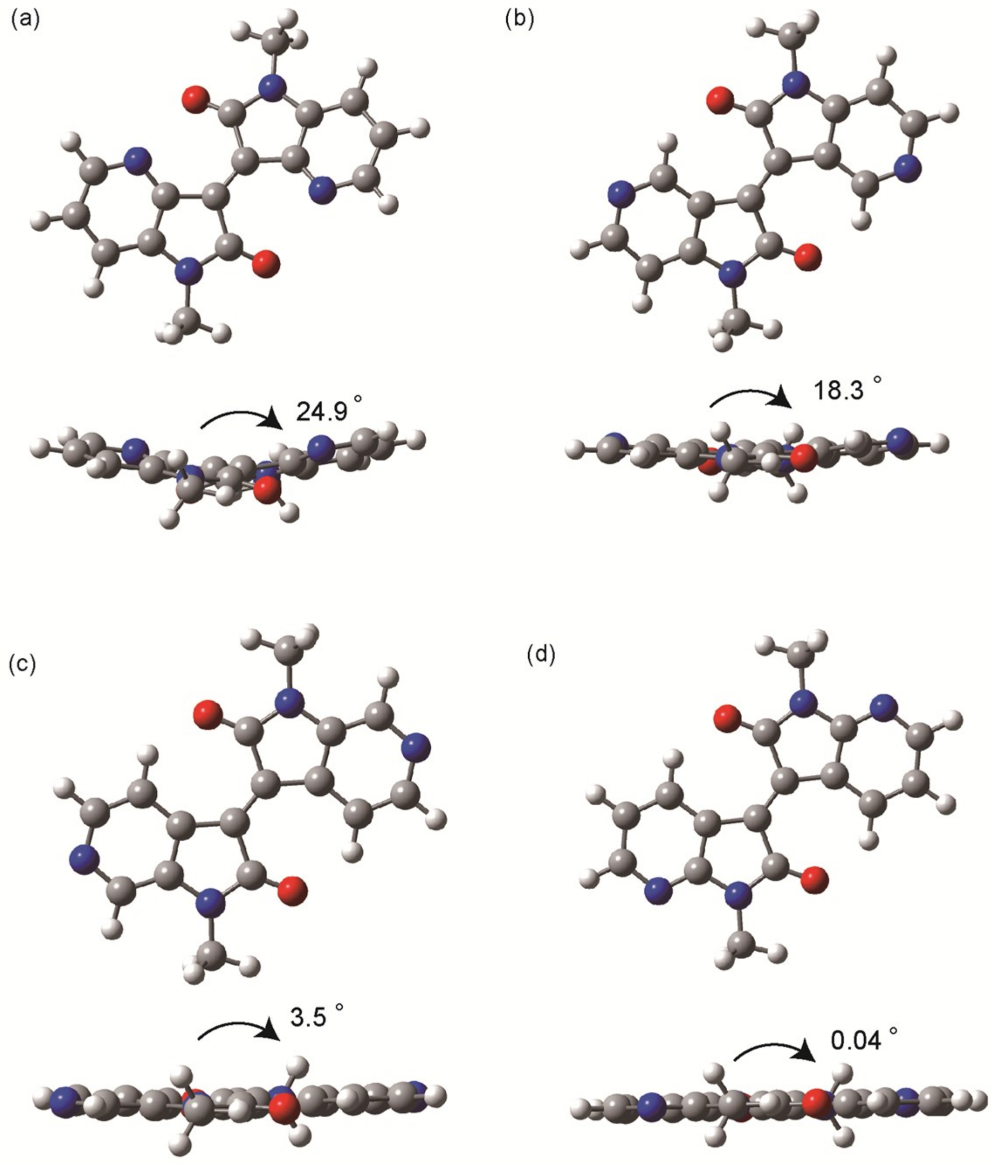

Fig. S1. Optimized molecular geometry depending on nitrogen positions on the diazaisoindigo core at (a) 4,4’-positions, (b) 5,5’-positions, (c) 6,6’-positions, and (d) 7,7’-positions.

III. Material Synthesis

6-Bromo-7-azaindole **1** was prepared according to the previous report.[2]

1-Hexyl-6-bromo-7-azaindole (2)

To a solution of 6-Bromo-7-azaindole (0.5 g, 2.54mmol) dissolved in dry DMF (10 ml), NaH (55wt% dispersion in oil, 0.16 g, 3.71 mmol) was added in one portion, and the solution was stirred at r.t. for 30 min. Hexylbromide (0.4 ml, 2.77 mmol) was added to the solution, and the mixture was stirred at r.t. for 12 h. The reaction mixture was poured into water, and the mixture was extracted with CH_2Cl_2 and was washed with brine. After drying over $MgSO_4$, the solvent was removed and the residue was purified by silica-gel chromatography eluting with CH_2Cl_2-hexane (2/1 = v/v) to provide **2** as a clear oil (1.15 g, 63%).

^{1}H NMR (300 MHz, $CDCl_3$, 25 ˚C): δ 7.73 (d, J = 8.4 Hz, 1H), 7.18 (dd, J = 5.1, 3.6 Hz, 2H), δ 6.43 (d, J = 3.6 Hz, 1H), 4.24 (t, J = 7.5 Hz, 2H) 1.90-1.80 (m, 4H), 1.45-1.25 (m, 6H), 0.87 (t, J = 6.6 Hz, 3H). ^{13}C NMR (300 MHz, $CDCl_3$, 25 ˚C): δ 146.99, 134.49, 130.70, 127.95, 119.13, 99.63, 44.57, 31.35, 30.22, 26.41, 22.51, 13.97, one aromatic peak is overlapped. MS (EI) *m/z*: 282 $[M]^+$.

1-Hexyl-3,3,6-tribromo-7-azaoxiindole (3)[3]

To a solution of **2** (0.45 g, 1.60 mmol) dissolved in tert-butanol (20 ml), pyridinium bromide perbromide (2.90 g, 7.40m mol) was added in small potions at r.t., and the mixture was stirred at r.t. for 12 h. The solvent removed under reduced pressure, and the residue was extracted with EtOAc and washed with brine. After drying over $MgSO_4$, the solvent was removed and the residue was purified by silica-gel chromatography eluting with CH_2Cl_2-hexane (2/1 = v/v) to provide **3** as a red oil (0.45 g, 62%).

^{1}H NMR (300 MHz, $CDCl_3$, 25 ˚C): δ 7.66 (d, J = 7.5 Hz, 1H), 7.28 (d, J = 7.8 Hz 1H), 3.83 (t, J = 7.5 Hz, 2H), 1.85-1.73 (m, 2H), 1.45-1.22 (m, 6H), 0.88 (t, J = 7.8 Hz, 3H). ^{13}C NMR (300 MHz, $CDCl_3$, 25 ˚C): δ 169.06, 152.53, 142.80, 134.83, 124.56, 123.09, 40.30, 31.21, 27.08, 26.11, 22.46, 13.96, one aromatic peak is overlapped. MS(EI) *m/z*: 454 $[M]^+$.

1-Hexyl-6-bromo-7-azaoxiindole (7a)

To a solution of **2** (1.20 g, 2.64 mmol) dissolved in acetic acid (20 ml), zinc dust (1.73 g,26.4 mmol) was added, and the mixture was stirred at r.t. for 12 h. The solvent was removed under reduced pressure, and the residue was extracted with EtOAc and washed with brine. After drying over $MgSO_4$, the solvent was removed to provide **7a** as a pale white solid (0.74 g, 95%), which was used without further purification.

^1H NMR (300 MHz, $CDCl_3$, 25 ˚C): δ 7.32 (d, J = 7.8 Hz, 1H), 7.11 (d, J = 7.8 Hz 1H), 3.78 (t, J = 7.5 Hz, 2H), 3.48 (s, 2H), 1.75-1.63 (m, 2H), 1.38-1.26 (m, 6H), 0.88 (t, J = 7.8 Hz, 3H). ^{13}C NMR (300 MHz, $CDCl_3$, 25 ˚C): δ 174.00, 158.42, 137.50, 133.32, 121.04, 111.66, 39.49, 34.46, 31.37, 27.51, 26.47, 22.54, 14.02. MS(EI) *m/z*: 296 $[M]^+$

1-Hexyl-6-bromo-7-azaisatin (8a)[5]

To a solution of **7a** (0.55g, 1.85 mmol) dissolved in dry DMSO (7 ml), *N*-bromosuccinimide (0.34 g, 1.92 mmol) was added at r.t., and the mixture was stirred under 60 °C for 12 h. The reaction mixture was poured into water, and the mixture was extracted with ethylacetate and was washed with brine. After drying over $MgSO_4$, the solvent was removed and the residue was purified by silica-gel chromatography eluting with CH_2Cl_2-hexane (2/1 = v/v) to provide **8a** as an oily orange solid (0.46 g, 80%).

^1H NMR (300 MHz, $CDCl_3$, 25 ˚C): δ 7.90 (d, J = 7.5 Hz, 1H), 7.27 (d, J = 7.5 Hz 1H), 3.83 (t, J = 7.5 Hz, 2H), 1.76-1.67 (m, 2H), 1.40-1.26 (m, 6H), 0.89 (t, J = 7.2 Hz, 3H). ^{13}C NMR (300 MHz, $CDCl_3$, 25 ˚C): δ 164.17, 158.10, 150.15, 133.97, 123.27, 110.25, 39.56, 31.25, 27.38, 26.41, 22.50, 13.98, one aromatic peak is overlapped. MS(EI) *m/z*: 311 $[M]^+$.

1,1'-Dihexyl-6,6'-dibromo-7,7'-diazaisoindigo (9a)

To a solution of **7a** (0.52 g, 1.75 mmol) and **8a** (0.50 g, 0.61 mmol) dissolved in acetic acid (15 ml), catalytic amount of conc. HCl 0.1 ml was added at r.t., and the mixture was stirred at 110 °C for 12 h. The resulting precipitate was filtered and washed with MeOH, H_2O, and hexane. After drying in vacuum, **9a** was obtained as a red solid (0.97 g, 94%).

^{1}H NMR (300 MHz, $CDCl_3$, 25 ˚C): δ 9.30 (d, J = 8.1 Hz, 2H), 7.22 (d, J = 8.1 Hz 2H), 3.87 (t, J = 7.2 Hz, 4H), 1.79-1.70 (m, 4H), 1.48-1.37 (m, 12H), 0.89 (t, J = 6.9 Hz, 6H). ^{13}C NMR (300 MHz, $CDCl_3$, 25 ˚C): δ 167.90, 157.81, 143.78, 139.09, 121.90, 114.50, 39.60, 31.36, 27.56, 26.52, 22.54, 14.02, one aromatic peak is overlapped. MS(MALDI-TOF) *m/z*: 590.81 $[M]^+$. Anal. Calcd for $C_{26}H_{30}Br_2N_4O_2$: C, 52.90; H, 5.12; N, 9.49; found: C, 52.92; H, 4.95; N, 9.45.

1,1'-dihexyl-6,6'-Dithienyl-7,7'-diazaisoindigo (6-6'-T-DAII)

The mixture of **9a** (0.12 g, 0.2 mmol), tributhylstanylthiophene (0.2 ml, 6.1 mmol), and Pd(dppf)Cl_2 (0.02 g, 0.028 mmol) dissolved in dry toluene (8 ml) was stirred to reflux for 24 h. The reaction mixture was poured into water, and the mixture was extracted with CH_2Cl_2 and was washed with brine. After drying over Na_2SO_4, the solvent was removed and the residue was purified by silica-gel chromatography eluting with CH_2Cl_2-hexane (2/1 = v/v) to provide **1** as a dark purple solid (0.09 g, 76%).

^{1}H NMR (300 MHz, $CDCl_3$, 25 ˚C): δ 9.44 (d, J = 8.4 Hz 2H), 7.71 (dd, J = 2.0, 1.5 Hz , 2H), 7.46 (dd, J = 2.5, 1.1 Hz, 2H), 7.36 (d, J = 8.4 Hz 2H), 7.15 (dd, J = 3.6, 2.4 Hz 2H), 3.97 (t, J = 7.7 Hz, 4H), 1.90-1.81

(m, 4H), 1.44-1.31 (m, 12H), 0.89 (t, *J* = 7.0 Hz, 6H). The ^{13}C NMR failed to obtain a spectrum because of the limited solubility of the product in chloroform. MS (MALDI-TOF) *m/z*: 597.46 [M+H]$^{+}$. Anal. Calcd for $C_{34}H_{36}N_4O_2S_2$: C, 68.43; H, 6.08; N, 9.39; found: C, 68.17; H,5.99; N, 9.28.

1-Hexyl-7-azaindole (5)

The compound **5** was prepared according to the same procedure for **1** using 7-azaindole (1.0 g, 8.46 mmol), NaH (55wt% dispersion in oil, 0.55 g, 12.4 mmol), and hexylbromide (1.4 ml, 9.23 mmol) to provide **5** as a clear oil (1.74 g, quant.).

^{1}H NMR (300 MHz, $CDCl_3$, 25 ˚C): δ 8.33-8.31 (m, 1H), 7.90-7.88 (m, 1H), 7.21 (d, *J* = 3.3 Hz, 1H), 7.06-7.02 (m, 1H), 6.44 (d, *J* = 3.3 Hz, 1H), 4.28 (t, *J* = 7.2 Hz, 2H), 1.92-1.82 (m, 2H), 1.45-1.22 (m, 6H), 0.86 (t, *J* = 6.9 Hz, 3H). ^{13}C NMR (300 MHz, $CDCl_{3,}$ 25 ˚C): δ 142.63, 128.61, 127.89, 120.52, 115.43, 99.13, 44.58, 31.42 30.38, 26.54, 26.52, 22.51, 13.97, one aromatic peak is overlapped. MS(EI) *m/z*: 202 [M]$^{+}$.

1-Hexyl-3,3,5-tribromo-7-azaoxiindole (6)[4]

To a solution of **6** (1.60 g, 7.91 mmol) dissolved in tert-butanol (20 ml) and H_2O (20 ml), bromine (16 g, 100 mmol) was added dropwise, and the mixture was stirred at r.t. for 12 h. The solvent was removed under reduced pressure, the residue was purified by silica-gel chromatography eluting with CH_2Cl_2-hexane (2/1 = v/v) to provide **6** as a red oil (3.24 g, 70%).

^{1}H NMR (300 MHz, $CDCl_3$, 25 ˚C): δ 8.31 (d, *J* = 8.1 Hz, 1H), 7.94 (d, *J* = 8.1 Hz, 1H), 3.82 (t, *J* = 7.2 Hz, 2H), 1.81-1.69 (m, 2H), 1.42-1.27 (m, 6H), 0.88 (t, *J* = 6.6 Hz, 3H). ^{13}C NMR (300 MHz, $CDCl_{3,}$ 25 ˚C): δ 168.69, 151.14, 150.87, 135.82, 127.18, 114.64, 40.30, 31.27 27.11, 26.18, 22.64, 14.11, one aromatic peak is overlapped. MS (MALDI-TOF) *m/z*: 451.16 $[M]^+$

1-Hexyl-5-bromo-7-azaoxiindole (7b)

The compound **7b** was prepared according to the same procedure for **7a** using **6** (3.10 g, 6.81mmol) and zinc dust (4.45 g, 68.1 mmol) to provide **7b** as a pale pink oil (2.02 g, quant.). ^{1}H NMR (300 MHz, $CDCl_3$, 25 ˚C): δ 8.25 (s, 1H), 7.59 (s, 1H), 3.81 (t, J = 7.5 Hz, 2H), 3.55 (s, 2H), 1.71-1.63 (m, 2H), 1.31-1.23 (m, 6H), 0.87 (t, J = 7.2 Hz, 3H). ^{13}C NMR (300 MHz, $CDCl_3$, 25 ˚C): δ 181.16, 174.60, 156.31, 144.80, 135.06, 124.20, 114.96, 39.51, 31.31, 27.40, 26.47, 22.48, 13.98. MS(EI) *m/z*: 296 $[M]^+$.

1-Hexyl-5-bromo-7-azaisatin (8b)[5]

The compound **8b** was prepared according to the same procedure for **8a** using **7b** (1.3 g, 4.37 mmol) and N-bromosuccinimide (0.81 g, 4.53 mmol) to provide **8b** as a dark red oily solid solid (0.28 g, 21%). ^{1}H NMR (300 MHz, $CDCl_3$, 25 ˚C): δ 8.52 (s, 1H), 7.91 (s, 1H), 3.83 (t, J = 7.2 Hz, 2H), 1.75-1.68 (m, 2H), 1.43-1.31 (m, 6H), 0.88 (t, J = 6.6 Hz, 3H). ^{13}C NMR (300 MHz, $CDCl_3$, 25 ˚C): δ 177.03, 173.70, 156.80, 147.40, 134.40, 120.92, 113.26, 39.52, 31.39, 27.54, 26.49, 22.50, 13.97. MS(EI) *m/z*: 310 $[M]^+$.

1,1'-Dihexyl-5,5'-dibromo-7,7'-diazaisoindigo (9b)

The compound **9b** was prepared according to the same procedure for **9a** using **7b** (0.27 g, 0.9 mmol) and **8b** (0.28 g, 0.9mmol) to provide **9b** as a red solid (0.31 g, 58%). ^{1}H NMR (300 MHz, $CDCl_3$, 25 ˚C): δ 9.66 (s, 1H), 8.33 (s, 1H), 3.88 (t, J = 6.9 Hz, 2H), 1.78-1.69 (m, 2H), 1.40-1.29 (m, 6H), 0.89 (t, J = 7.2 Hz, 3H). ^{13}C NMR (300 MHz, $CDCl_3$, 25 ˚C): δ 166.96, 156.41, 151.14, 139.95, 132.21, 117.07, 113.91, 39.64, 31.46, 27.62, 26.60, 22.56, 14.03. MS (MALDI-TOF) *m/z*: 590.07 $[M]^+$. Anal. Calcd for

$C_{26}H_{30}Br_2N_4O_2$: C, 52.90; H, 5.12; N, 9.49; found: C, 52.88; H, 4.88; N, 9.43.

1,1'-Dihexyl-5,5'-dithienyl-7,7'-diazaisoindigo (5-5'-T-DAII)

The compound **5-5'-T-DAII** was prepared according the same procedure for **6-6'-T-DAII** using **9b** (0.12 g, 0.20 mmol), tributhylstanylthiophene (0.2 ml, 6.1 mmol), $Pd(PPh_3)_4$ (0.02 g, 0.02 mmol) to provide **1** as a purple solid (0.09 g, 75%).

^1H NMR (300 MHz, $CDCl_3$, 25 ˚C): δ 9.82 (d, *J* = 2.2 Hz, 2H), 8.51 (d, *J* = 1.8 Hz, 2H), 7.39 (dd, *J* = 1.8, 1.5 Hz, 2H), 7.33 (dd, *J* = 2.6, 1.1 Hz, 2H), 7.137 (dd, *J* = 3.7, 2.6 Hz, 2H), 3.94 (t, *J* = 7.3 Hz, 4H), 1.85-1.72 (m, 4H), 1.46-1.32 (m, 12H), 0.89 (t, *J* = 7.0 Hz, 6H). The ^{13}C NMR failed to obtain a spectrum because of the limited solubility of the product in chloroform. MS (MALDI-TOF) *m/z*: 597.49 $[M+H]^+$. Anal. Calcd for $C_{34}H_{36}N_4O_2S_2$: C, 68.43; H, 6.08; N, 9.39; found: C, 68.49; H, 6.02; N, 9.01.

^1H NMR spectra for compound **9a**

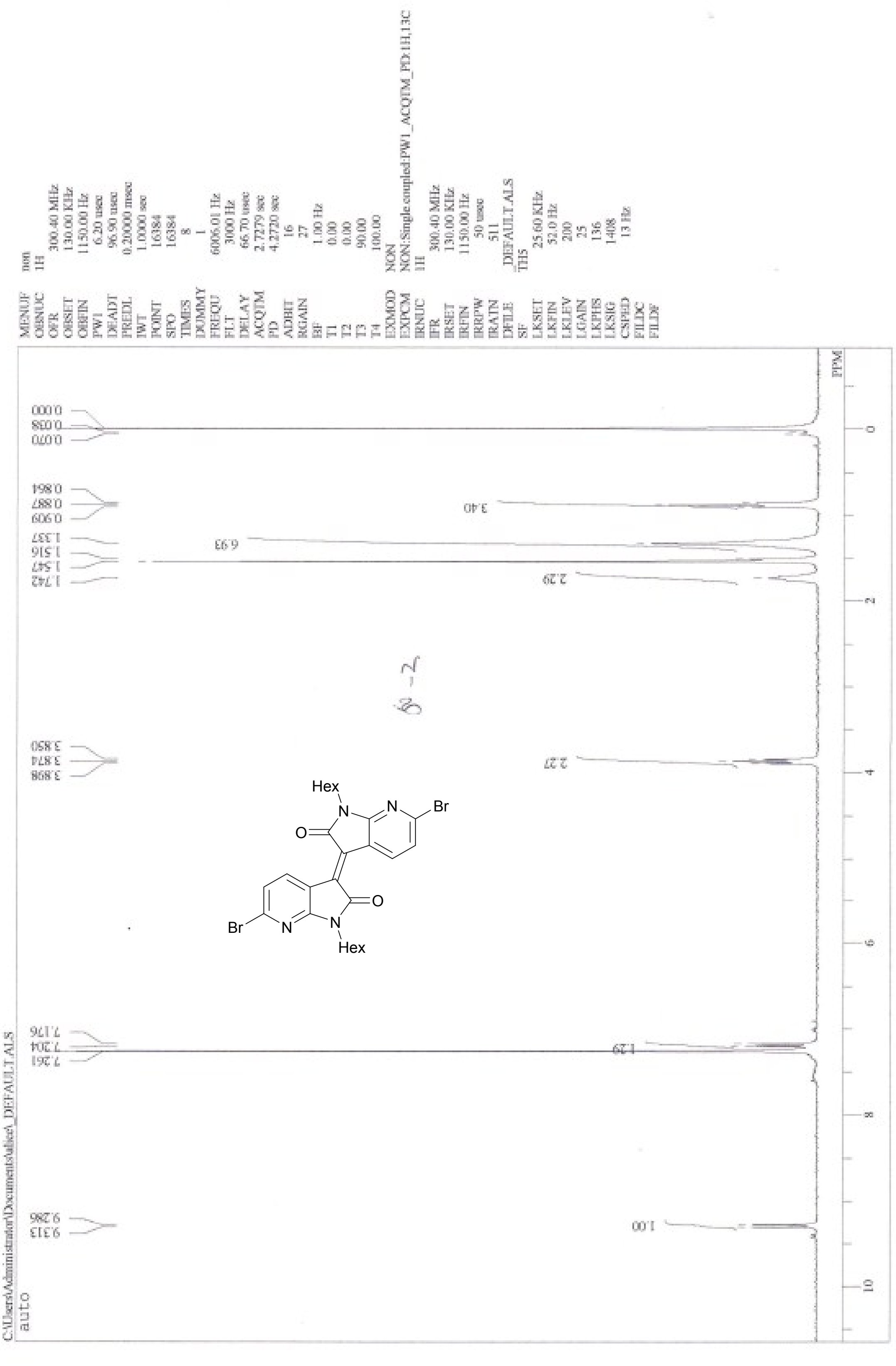

MENUF non
OBNUC 1H
OFR 300.40 MHz
OBSET 130.00 KHz
OBFIN 1150.00 Hz
PW1 6.20 usec
DEADT 96.90 usec
PREDL 0.20000 msec
IWT 1.0000 sec
POINT 16384
SPO 16384
TIMES 8
DUMMY 1
FREQU 6006.01 Hz
FLT 3000 Hz
DELAY 66.70 usec
ACQTM 2.7279 sec
PD 4.2720 sec
ADBIT 16
RGAIN 27
BF 1.00 Hz
T1 0.00
T2 0.00
T3 90.00
T4 100.00
EXMOD NON
EXPCM NON:Single coupled:PW1_ACQTM_PD:1H,13C
IRNUC 1H
IFR 300.40 MHz
IRSET 130.00 KHz
IRFIN 1150.00 Hz
IRRPW 50 usec
IRATN 511
DFILE _DEFAULT.ALS
SF TH5
LKSET 25.60 KHz
LKFIN 52.0 Hz
LKLEV 200
LGAIN 25
LKPHS 136
LKSIG 1408
CSPED 13 Hz
FILDC
FILDF

^{13}C NMR spectra for compound **9a**

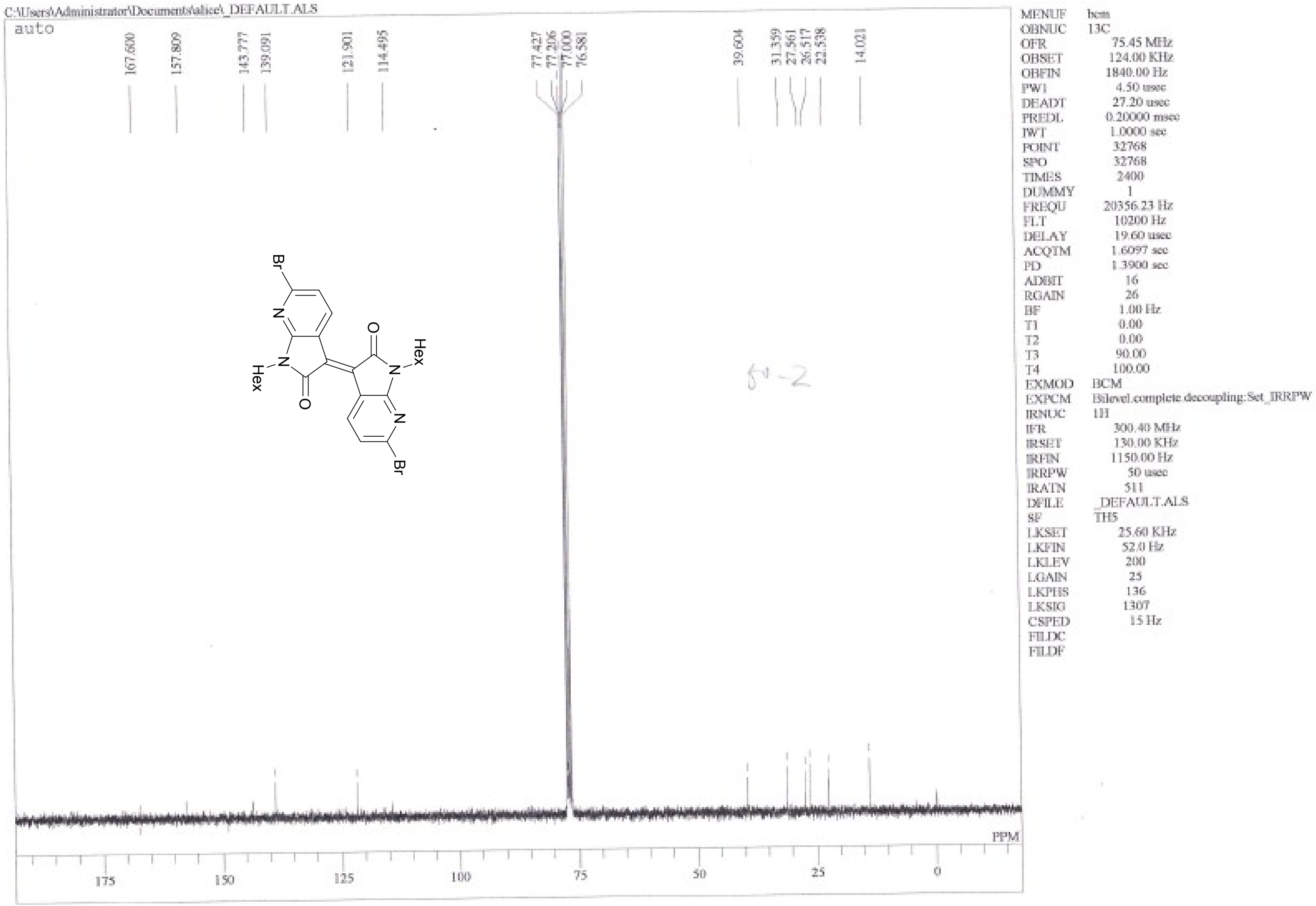

```
MENUF     bcm
OBNUC     13C
OFR           75.45 MHz
OBSET        124.00 KHz
OBFIN       1840.00 Hz
PW1            4.50 usec
DEADT         27.20 usec
PREDL        0.20000 msec
IWT          1.0000 sec
POINT         32768
SPO           32768
TIMES          2400
DUMMY             1
FREQU      20356.23 Hz
FLT           10200 Hz
DELAY         19.60 usec
ACQTM        1.6097 sec
PD           1.3900 sec
ADBIT            16
RGAIN            26
BF             1.00 Hz
T1             0.00
T2             0.00
T3            90.00
T4           100.00
EXMOD     BCM
EXPCM     Bilevel.complete.decoupling:Set_IRRPW
IRNUC     1H
IFR          300.40 MHz
IRSET        130.00 KHz
IRFIN       1150.00 Hz
IRRPW            50 usec
IRATN           511
DFILE     _DEFAULT.ALS
SF        TH5
LKSET         25.60 KHz
LKFIN          52.0 Hz
LKLEV           200
LGAIN            25
LKPHS           136
LKSIG          1307
CSPED            15 Hz
FILDC
FILDF
```

MS chart for compound **9a**

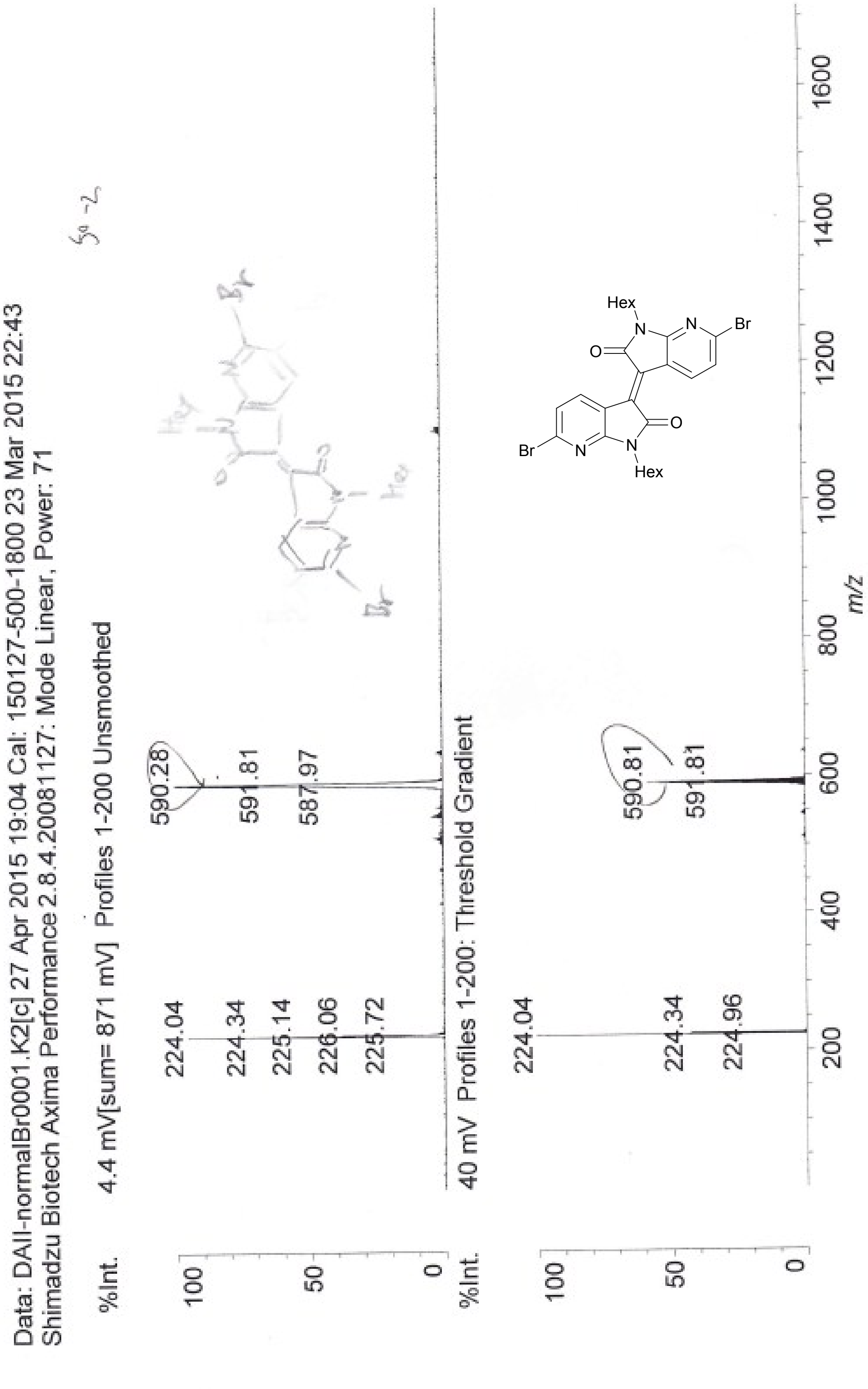

^{1}H NMR spectra for **6-6’-T-DAII**

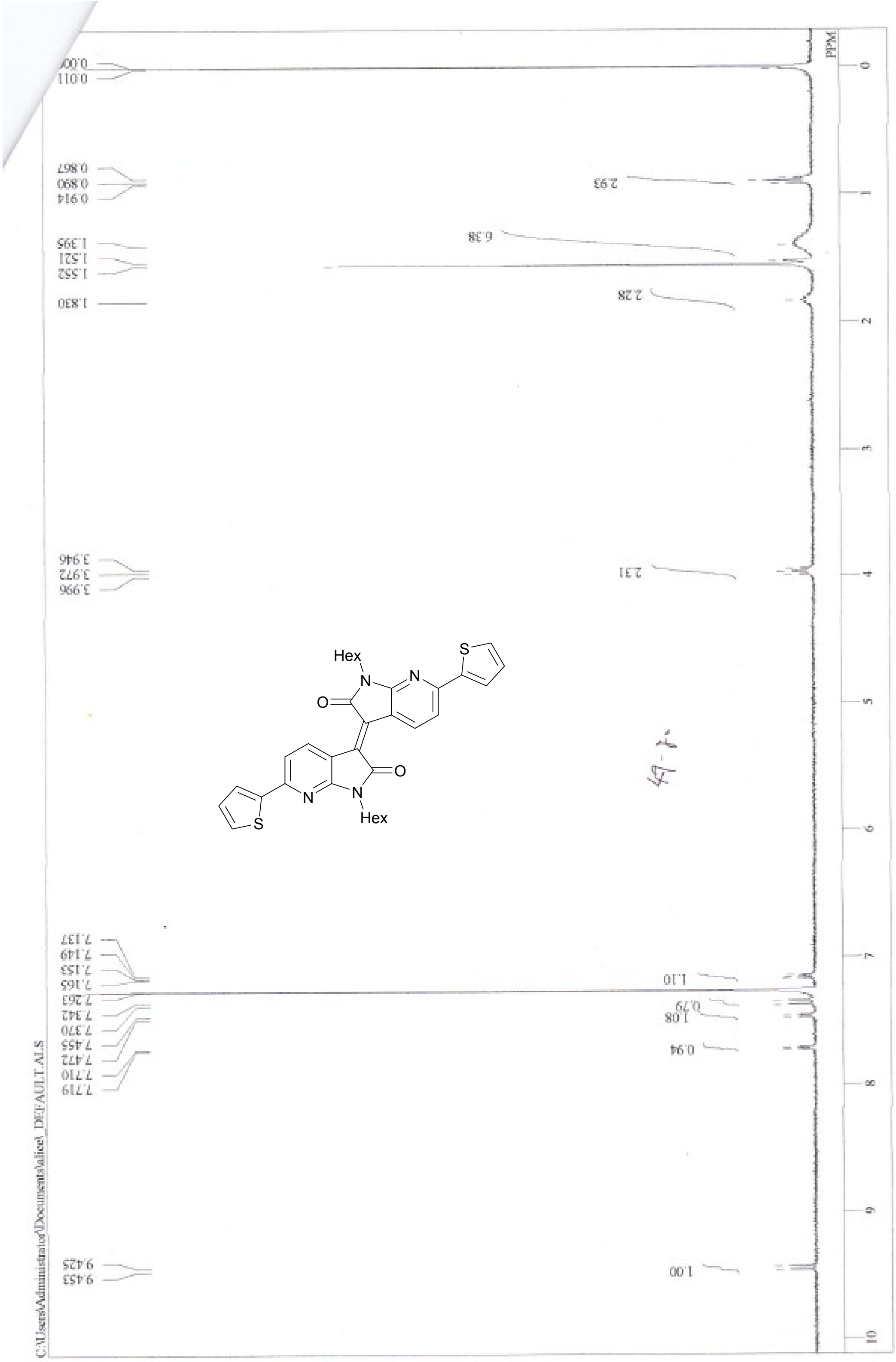

MS chart for **6-6’-T-DAII**

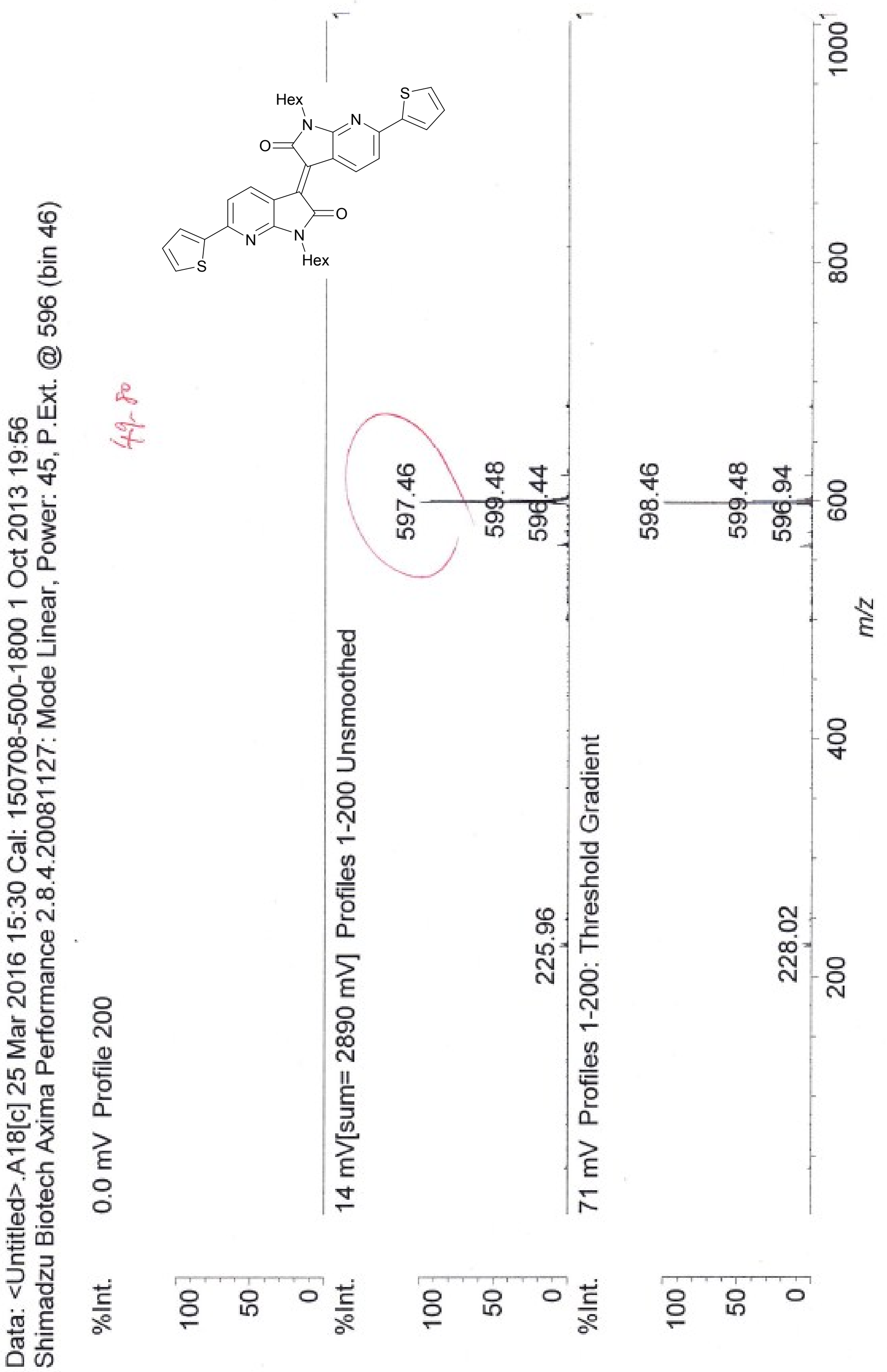

^{1}H NMR spectra for compound **9b**

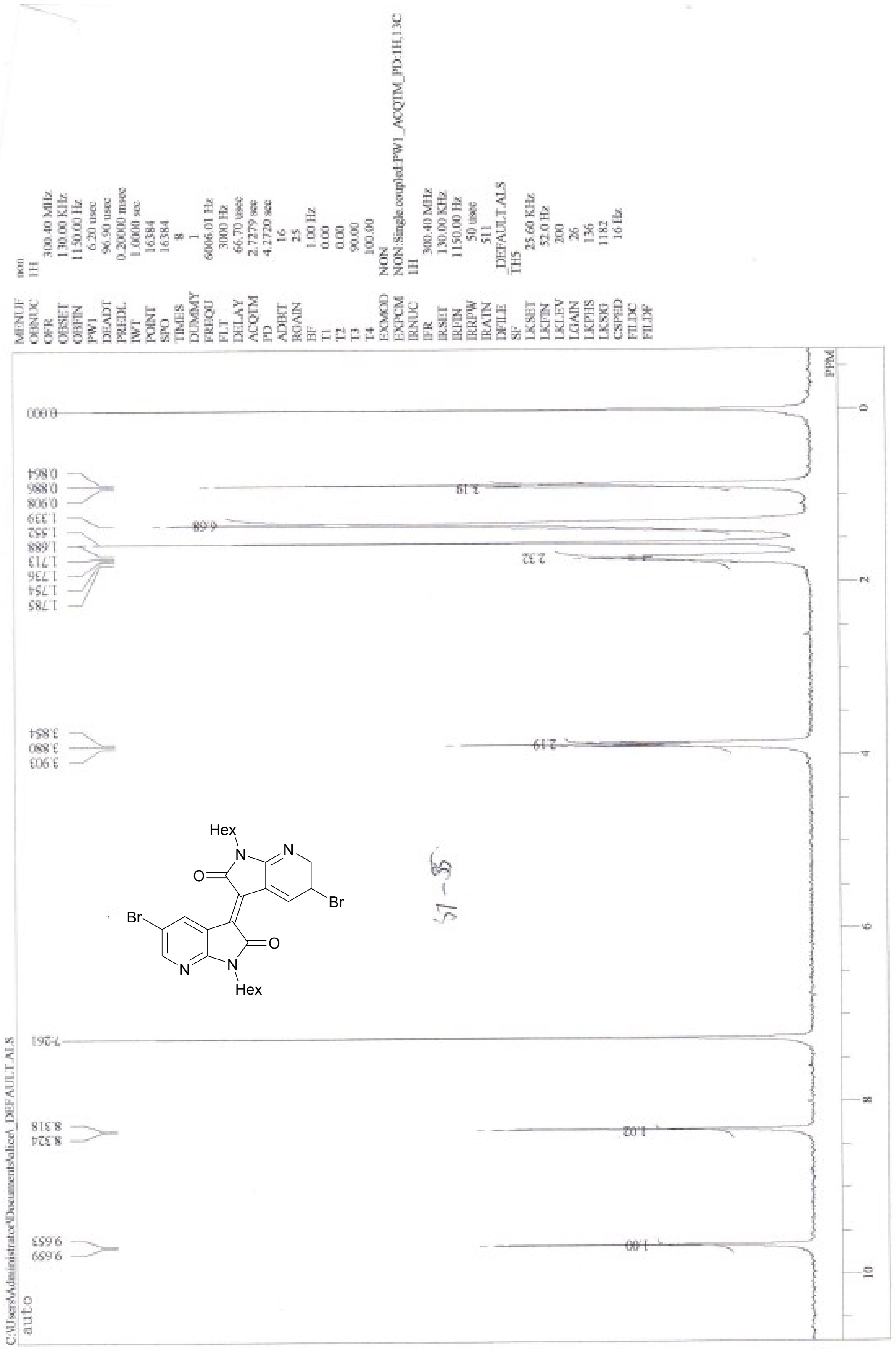

^{13}C NMR spectra for compound **9b**

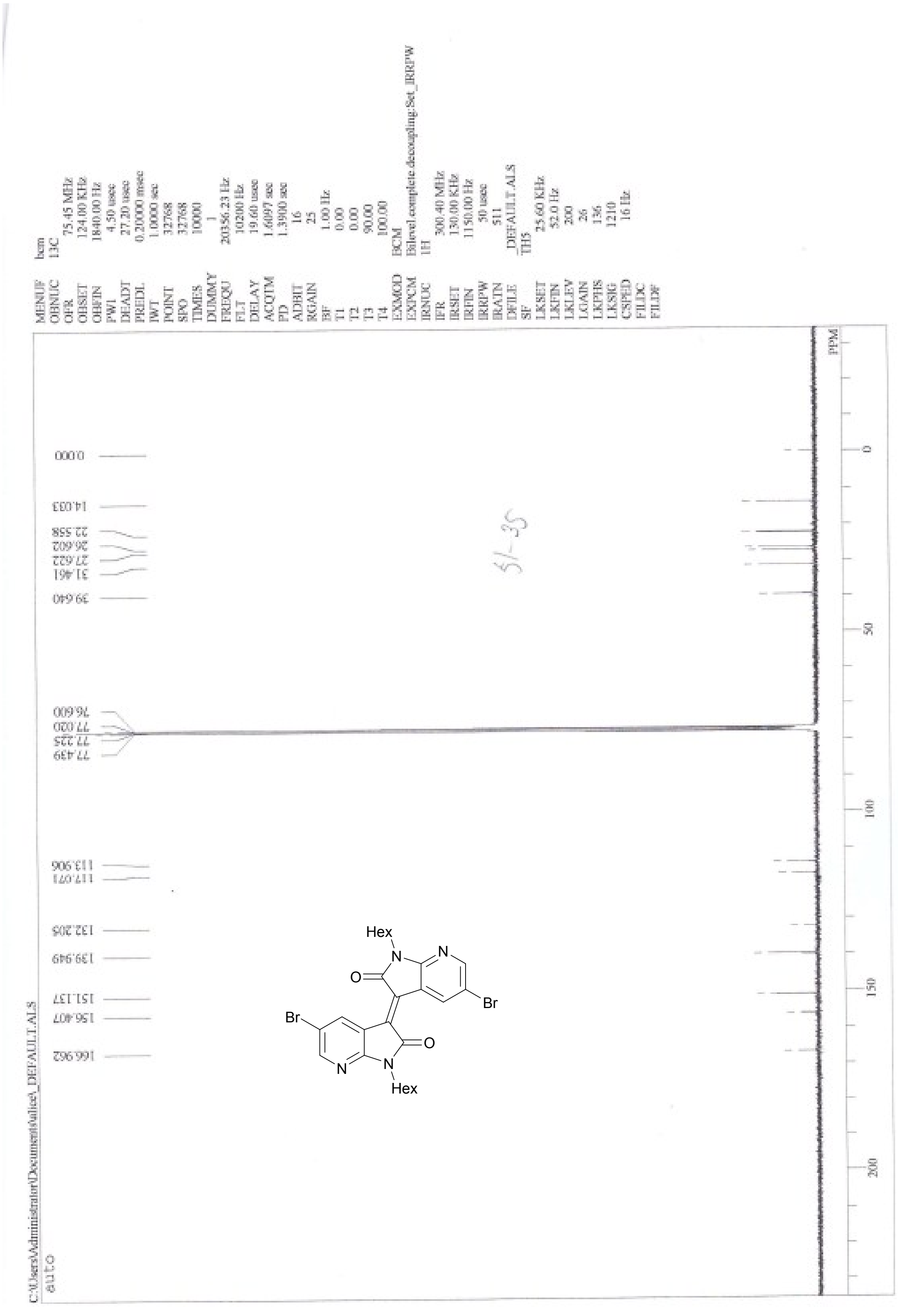

MS chart for compound **9b**

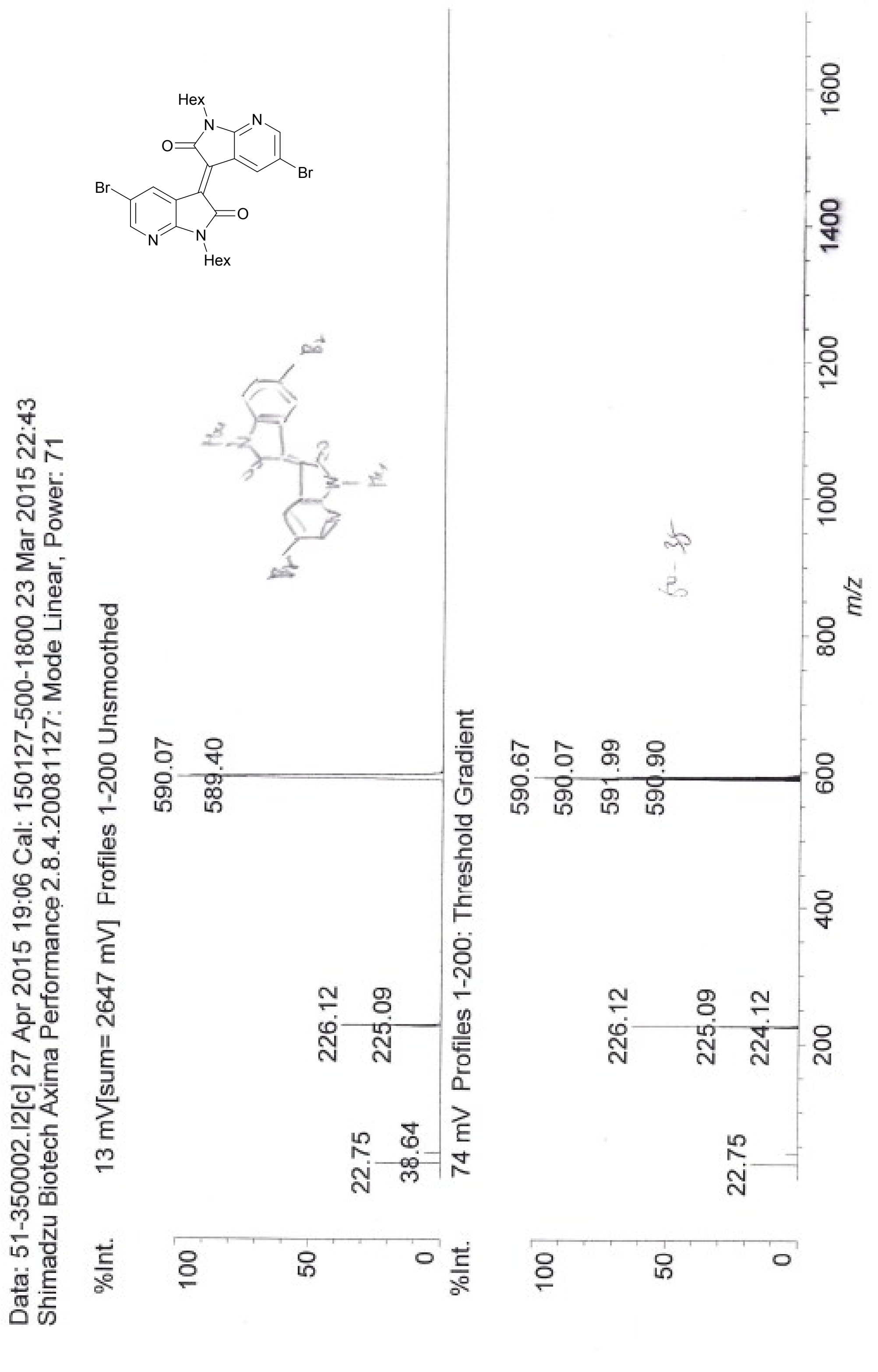

^{1}H NMR spectra for **5-5'-T-DAII**

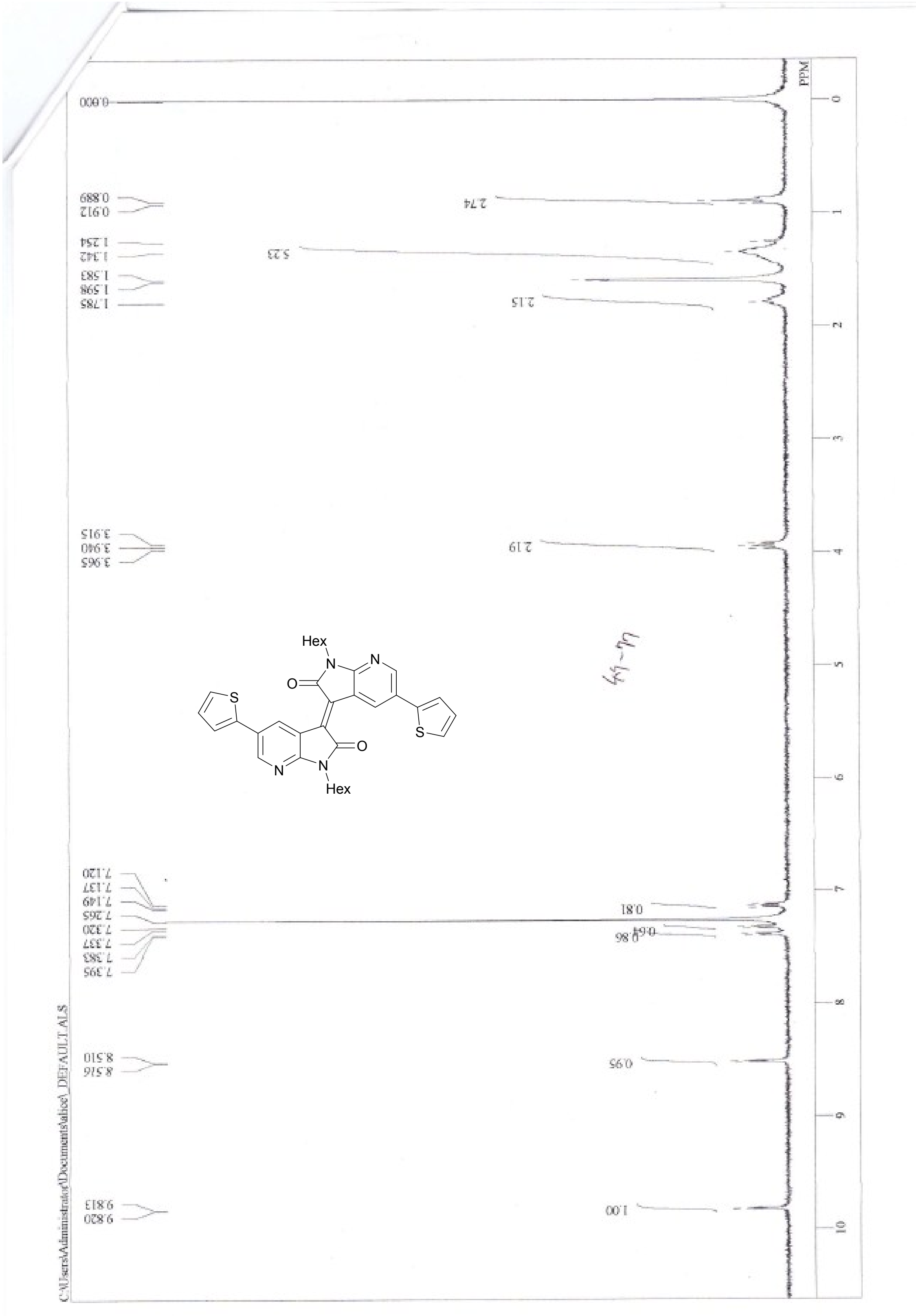

MS chart for **5-5’-T-DAII**

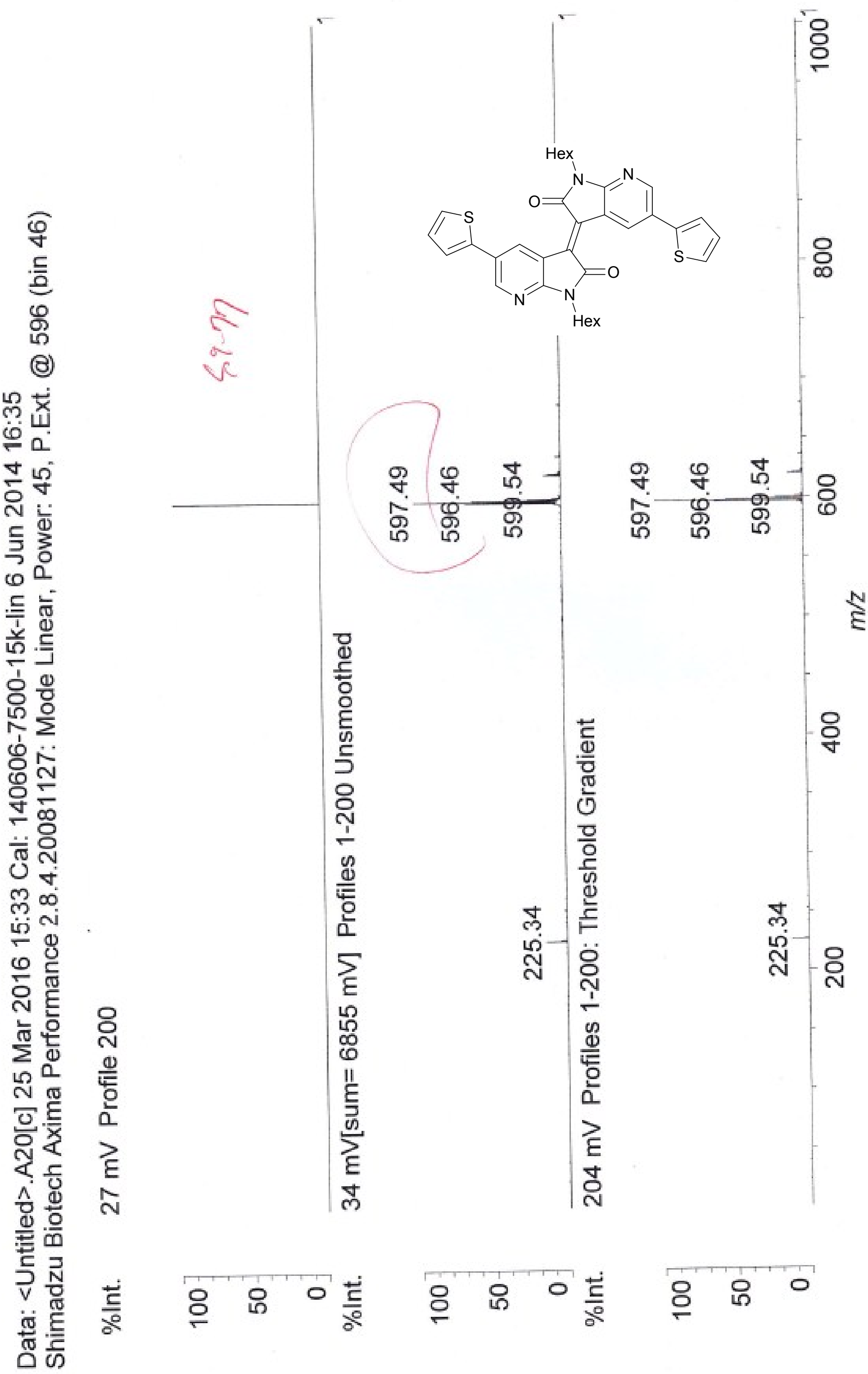

IV. Thermal properties

Thermal gravimetric analyses (TGA) were performed using a RIGAKU Thermo plus EVO TG8120 thermal analyzer at the heating rate of 10 ˚C min^{-1} under a N_2 atmosphere. Differential scanning calorimetric (DSC) measurements were performed with an SII EXSTAR DSC-6100 at the heating rate of 5 ˚C min^{-1} under a N_2 atmosphere. For the DSC measurements, the second heating-cooling cycles were analyzed.

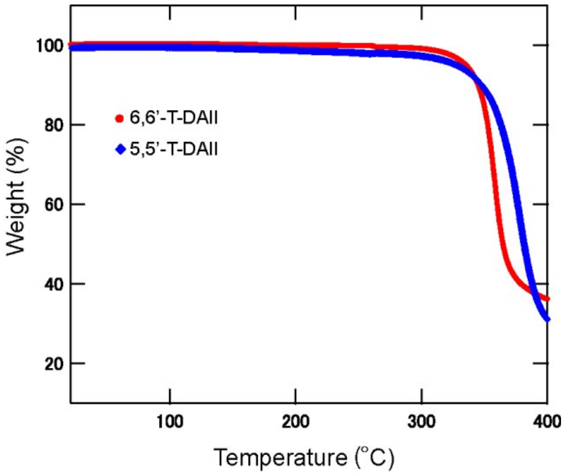

Fig. S2. TGA curves of **6,6’-T-DAII and 5,5’-T-DAII** at the heating rate of 10 ˚C / min under N_2 atmosphere.

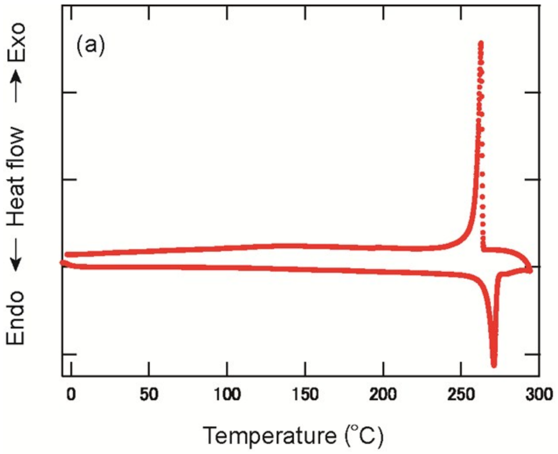

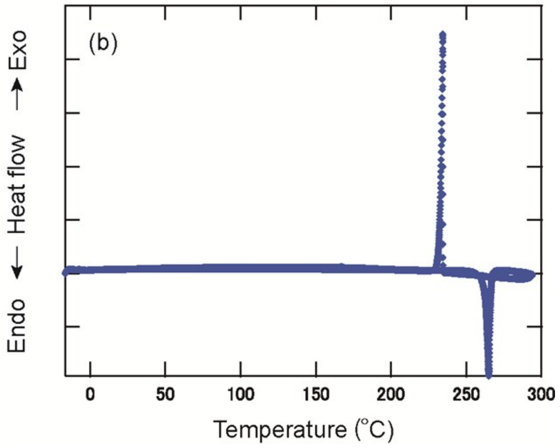

Fig. S3. DSC curves of **6,6'-T-DAII and 5,5'-T-DAII** at the heating rate of 5 ˚C / min under N_2 atmosphere.

V. X-ray Single Crystal Structure Analysis

The crystal structures were determined from single-crystal X-ray diffraction data. The measurements were made by a RIGAKU R-AXIS RAPID II imaging plate with Cu-Kα radiation from a rotation anode source with a confocal multilayer X-ray mirror (RIGAKU VM-spider, λ = 1.54187 Å). The diffraction data were corrected under -100 °C. The structures were solved by the direct method (SHELX-97).[6] The structures were refined by the full-matrix least-squares procedure by applying anisotropic temperature factors. The positions of the hydrogen atoms were calculated. The disordered sulfur and carbon atoms of **6,6’-T-DAII** are analyzed population analysis.

Table S1 Crystallographic data

	9a	**6-6’-T-DAII**	**5-5’-T-DAII**
Chemical formula	$C_{26}H_{30}Br_2N_4O_2$	$C_{34}H_{36}N_4O_2S_2$	$C_{34}H_{36}N_4O_2S_2$
Crystal System	monoclinic	triclinic	monoclinic
Formura weight	590.36	596.80	596.80
Shape	red block	black needle	brown plate
Space group	$P2_1/n$	$P(-1)$	$P2_1/c$
a / Å	4.64320(8)	5.02134(9)	14.00800(15)
b / Å	34.6471(7)	9.79352(18)	5.00611(6)
c / Å	7.77338(14)	16.0988(3)	21.3879(3)
α / °		99.8742(10)	
β / °	93.4634(9)	98.6417(11)	104.3730(12)
γ / °		101.4850(10)	
V / Å^3	1248.25(4)	750.27(2)	1452.89(3)
Z	2	1	2
D_{calc} / g cm^{-3}	1.571	1.321	1.364
Data / parameters	2297/154	2692/228	2847/191
Goodness of fit on F^2_0	0.945	1.158	1.056
R_1[a] /Rw[b]	0.04750.1460	0.0520/0..1362	0.0502/0.1359

[a] $R_1 = \Sigma\|F_0| - |F_c\|/\Sigma|F_0|$ · [b] $R_w = [\Sigma w(|F_0| - |F_c|)^2 / \Sigma wF_0^2]^{1/2}$

VI. Electrochemical properties

Cyclic voltammetry (CV) was carried out using an ALS/CH Instruments Electrochemical Analyzer Model 700C. The measurement was performed in dehydrated dichloromethane solution containing 0.1 M *n*-Bu_4NPF_6 as the supporting electrolyte using a glassy carbon working electrode, a platinum counter electrode, and an $Ag/AgNO_3$ electrode as a reference electrode at the scan rate of 100 mV s^{-1}. The films of the present compounds were formed on a glassy carbon working electrode. From the onset reduction potentials and $E_{\mathrm{red,\ onset}}$, LUMO levels were estimated by assuming the ferrocene/ferrocenium energy level to be -4.8 eV under the vacuum level.[7] The HOMO levels are estimated from the LUMO value and the optical bandgap.

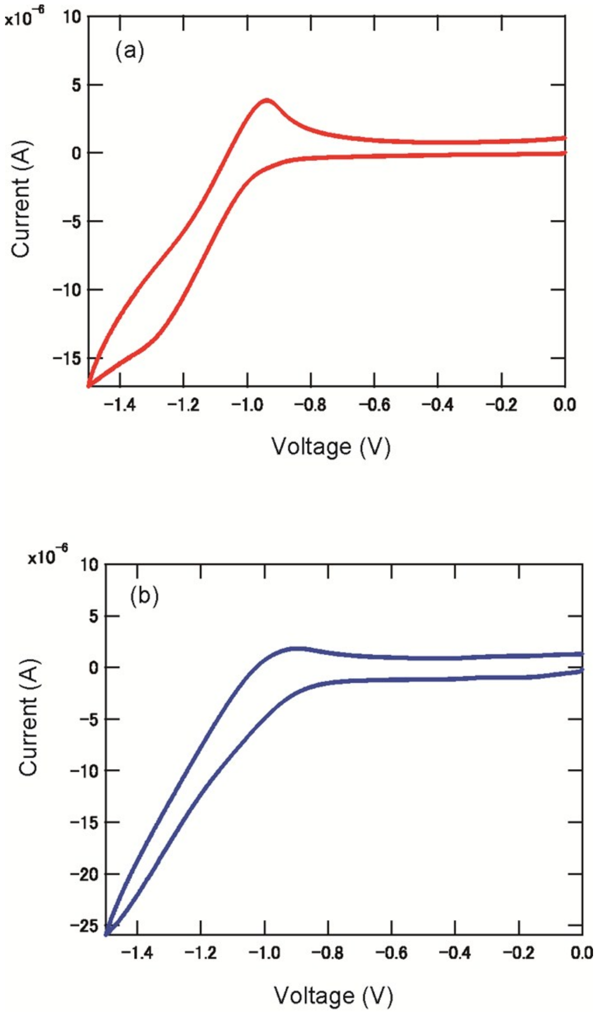

Fig. S4. Cyclic voltamograms of (a) **6,6'-DAII** and (b) **5,5'-DAII.** In the positive scan, no noticeable peaks were observed.

VIII. Transistor fabrication and thin-film characterization

A 300-nm thermally grown SiO_2 on a highly-doped silicon wafer (capacitance (C_i) = 11.5 nF cm^{-2}) was cleaned in a piranha solution (70% H_2SO_4 + 30% H_2O_2) for 15 min, and then washed with distilled water. [6] As a gate insulator layer, the TTC was thermally evaporated to form a 20-nm-thick TTC layer on the Si substrate. The active layer was formed by thermal deposition under a vacuum of ca. 1.0×10^{-4} Pa, in which the resulting thickness was 45 nm. Finally, the source and drain electrodes were formed by the vapor deposition of Au (50 nm). The standard channel length (L) and width (W) were 50 μm and 1000 μm, respectively. The organic field-effect transistor (OFET) properties were measured by a Keithley 4200 semiconductor parameter analyzer under vacuum conditions. The field-effect mobility (μ) and threshold voltage (V_{th}) were calculated in the saturation region using the equation, $I_{\mathrm{DS}} = \mu(WC_{\mathrm{i}}/2L)(V_{\mathrm{G}} - V_{\mathrm{th}})^2$, where I_{DS} and V_{G} are the drain current and gate voltage, respectively. The capacitance including the TTC layer on the SiO_2 substrate was calculated to be 1.25×10^{-8} F cm^{-2}.[8, 9,] Atomic force microscopic (AFM) images were obtained using an SII Nanonavi SPA400 scanning probe microscope with an SII SI-DF40 cantilever. Two-dimensional grazing incidence wide-angle X-ray scattering (GIWAXS) patterns were obtained at SPring-8 on beamline BL45XU. The samples were irradiated at a fixed incident angle on the order of 0.10 ° and the GIWAXS patterns were recorded with a 2-D image detector (PILATUS3X 2M). The wavelength of the X-ray beam was 0.1 nm (energy of 12.39 KeV) and the camera length was 395 mm.

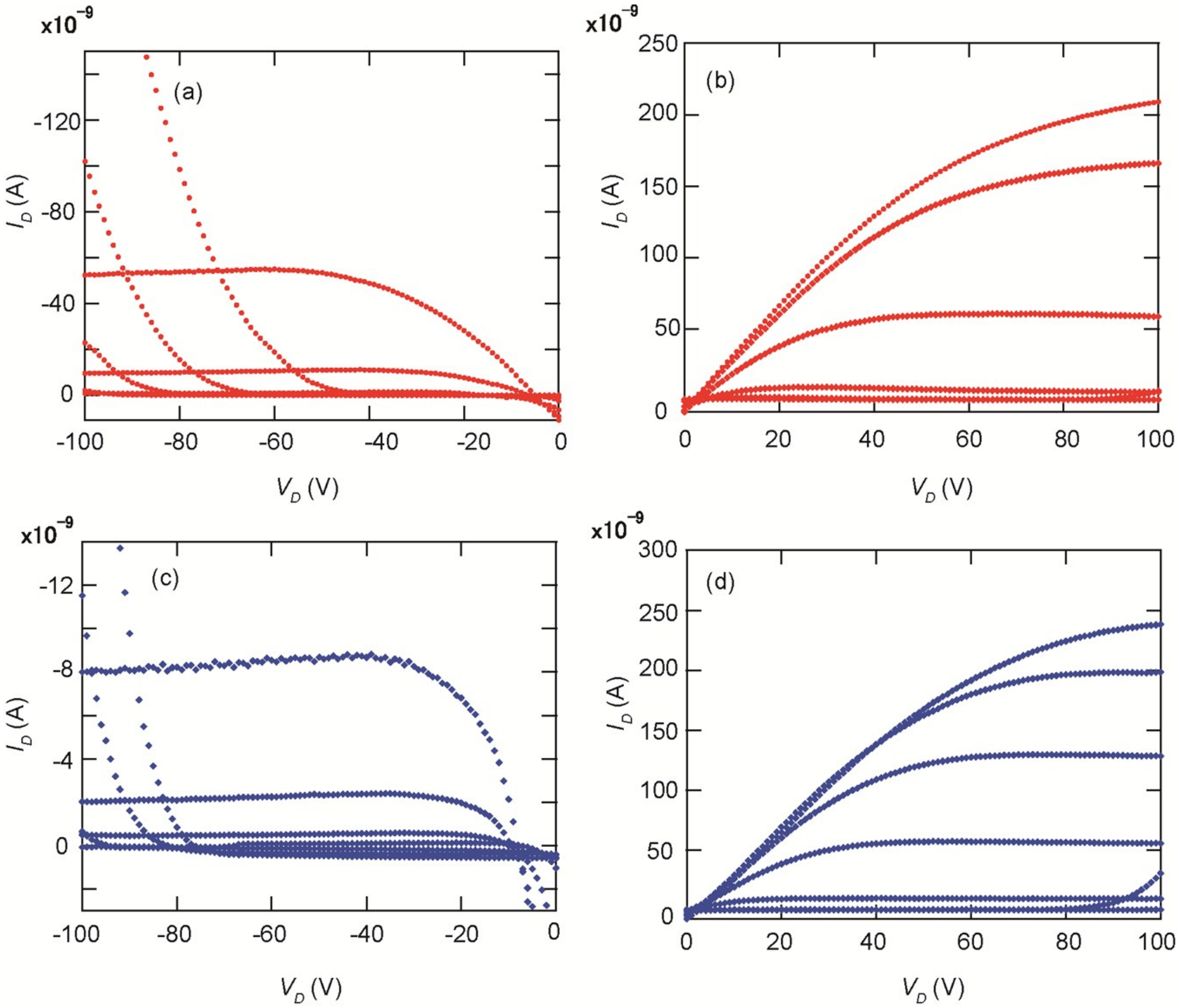

Figure S4. Typical output curves of (a) and (c) p-channel and (b) and (d) n-channel ((a) and (b) for **6,6'-T-DAII** and (c) and (d) for **5,5'-T-DAII**). Gate voltages (V_g) are changed from 20 V to -100 V for p-channel scan and from -20 V to 100 V for n-channel scan with 20 V steps.

References

1. M. J. Frisch, G. W. Trucks, H. B. Schlegel, G. E. Scuseria, M. A. Robb, J. R. Cheeseman, G. Scalmani, V. Barone, B. Mennucci, G. A. Petersson, H. Nakatsuji, M. Caricato, X. Li, H. P. Hratchian, A. F. Izmaylov, J. Bloino, G. Zheng, J. L. Sonnenberg, M. Hada, M. Ehara, K. Toyota, R. Fukuda, J.

Hasegawa, M. Ishida, T. Nakajima, Y. Honda, O. Kitao, H. Nakai, T. Vreven, J. A. Montgomery Jr, J. E. Peralta, F. Ogliaro, M. Bearpark, J. J. Heyd, E. Brothers, K. N. Kudin, V. N. Staroverov, R. Kobayashi, J. Normand, K. Raghavachari, A. Rendell, J. C. Burant, S. S. Iyengar, J. Tomasi, M. Cossi, N. Rega, N. J. Millam, M. Klene, J. E. Knox, J. B. Cross, V. Bakken, C. Adamo, J. Jaramillo, R. Gomperts, R. E. Stratmann, O. Yazyev, A. J. Austin, R. Cammi, C. Pomelli, J. W. Ochterski, R. L. Martin, K. Morokuma, V. G. Zakrzewski, G. A. Voth, P. Salvador, J. J. Dannenberg, S. Dapprich, A. D. Daniels, ¨O. Farkas, J. B. Foresman, J. V. Ortiz, J. Cioslowski and D. J. Fox, The molecular orbital calculation was carried out using the Gaussian 09, Revision B.01, Gaussian, Inc., Wallingford CT, 2009.

2. S. Minakata, M. Komatsu, and Y. Ohshiro, *Synthesis*, **1992**, 661-663.
3. X. K. Wee, T. Yang, and M. L. Go, *ChemMedChem*., **2012**, 777-791.
4. P. W. Wu, Y. M. Cheng, W. T. Hsieh, Y. H. Wang, C. Y. Wei, and P. T. Chou, *ChemMedChem*., **2007**, 1071-1075.
5. X. Cheng, K. -H. Merz, S. Vatter, J. Christ, and S. Wölfi, *Bioorg. Med. Chem*., **2014**, 247-255.
6. G. M. Sheldrick, *Acta Crystallogr., Sect. A: Found. Crystallogr*., 2008, **64**, 112-122.
7. B. W. D'Andrade, S. Datta, S. R. Forrest, P. Djurovich, E. polikarpov, and M. E. Thompson, *Org. Electron*, 2005, **6**, 11-20.
8. M. Kraus, S. Richler, A. Opitz, W. Brutting, S. Haas, T. Hasegawa, A. Hinderhofer and F. Schreiber. *J. Appl. Phys*., 2010, **107**, 094503.

9. K. J. Baeg, Y. Y. Noh, J. Ghim, B. Lim and D. Y. Kim, *Adv. Funct. Mater.*, 2008, **18**, 3678–3685.